STEM CELLS®

EMBRYONIC STEM CELLS/INDUCED PLURIPOTENT STEM CELLS

Activation-Induced Cytidine Deaminase Regulates Fibroblast Growth Factor/Extracellular Signal-Regulated Kinases Signaling to Achieve the Naïve Pluripotent State During Reprogramming

RITU KUMAR, TODD EVANS *

Key Words. iPSCs • DNA methylation • Epigenetics • Mitogen-activated protein kinase signaling

Department of Surgery, Weill Cornell Medicine, New York, New York, USA

*Lead contact author

Correspondence: Ritu Kumar, Ph.D., Department of Surgery, Weill Cornell Medicine, 1300 York Ave. LC-711, New York, New York, USA. Telephone: (212) 746-9487; e-mail: rik2002@med.cornell.edu; or Todd Evans, Ph.D., Department of Surgery, Weill Cornell Medicine, 1300 York Ave. LC-711, New York, New York, USA. Telephone: (212) 746-9485; e-mail: tre2003@med.cornell.edu

Received September 12, 2018; accepted for publication March 31, 2019; first published online April 25, 2019.

http://dx.doi.org/10.1002/stem.3023

ABSTRACT

Induced pluripotent stem cells (iPSCs) derived by in vitro reprogramming of somatic cells retain the capacity to self-renew and to differentiate into many cell types. Pluripotency encompasses multiple states, with naïve iPSCs considered as ground state, possessing high levels of self-renewal capacity and maximum potential without lineage restriction. We showed previously that activation-induced cytidine deaminase (AICDA) facilitates stabilization of pluripotency during reprogramming. Here, we report that *Acida*$^{-/-}$ iPSCs, even when successfully reprogrammed, fail to achieve the naïve pluripotent state and remain primed for differentiation because of a failure to suppress fibroblast growth factor (FGF)/extracellular signal-regulated kinases (ERK) signaling. Although the mutant cells display marked genomic hypermethylation, suppression of FGF/ERK signaling by AICDA is independent of deaminase activity. Thus, our study identifies AICDA as a novel regulator of naïve pluripotency through its activity on FGF/ERK signaling. STEM CELLS *2019;37:1003–1017*

SIGNIFICANCE STATEMENT

Growth factor signaling requirements that modulate pluripotent state are well studied. However, the epigenetic basis of how the dynamic state of pluripotent cells is regulated and stabilized is largely a black box. The current study is important because the results show that AICDA is essential for reprogramming to ground state. A better understanding for how to stabilize ground state pluripotent cells is of fundamental importance for the use of pluripotent cell sources in disease modeling and potential cellular therapies.

INTRODUCTION

Pluripotent stem cells (PSCs) can be derived from undifferentiated early embryonic blastomeres or by in vitro reprogramming of differentiated somatic cells by ectopic expression of several pluripotency-associated transcription factors. Provided defined culture conditions, PSCs can be propagated indefinitely in vitro. PSCs can differentiate into all the cell lineages of an embryo with little or no contribution to the extra-embryonic lineages [1]. The two most clearly defined states are the ground or naïve state, exemplified by mouse ESCs derived from the inner cell mass of preimplantation blastocysts and the primed state represented by human ESCs or mouse epiblast stem cells (EpiSCs) derived from postimplantation blastocysts. The distinguishing features of naïve or primed stem cells include colony morphology, relative expression levels of pluripotency and early differentiation genes, growth factor requirements for self-renewal, DNA methylation patterns, histone modification patterns, and X chromosome inactivation in female cells [1].

Reprogramming of somatic cells to induced PSCs (iPSCs) by ectopic expression of "Yamanaka" transcription factors has strongly impacted the field of stem cell biology and regenerative medicine, providing unlimited access of patient-specific stem cells for disease modeling, drug testing, and perhaps eventually autologous cellular therapies [2]. During reprogramming, a somatic cell is induced to undergo progressive transcriptomic and epigenomic alterations until arriving at a pluripotent state similar to ESCs [3, 4]. The iPSCs are functionally similar to ESCs in terms of the capacity to differentiate into cells representing any of the three germ layers, yet in some cases, their molecular profile has been described as distinct from ESCs, based on global gene expression comparisons of many ESC and iPSC lines [5, 6]. During

the extended and relatively inefficient reprogramming process, some iPSCs are clearly distinct from ESCs, because they fail to undergo complete reprogramming, never achieving ground state pluripotency, caught in a partially reprogrammed state. Such partially reprogrammed cells show reactivation of a distinct subset of stem-cell-related genes, incomplete repression of lineage-specifying transcription factors, and DNA hypermethylation at pluripotency-related loci [4]. Partially reprogrammed iPSCs may retain epigenetic marks of their cellular origin, whereas continued passaging under defined cell culture conditions may select for cells that stabilize a fully reprogrammed state [7].

Activation-induced cytidine deaminase (AICDA) is a member of the APOBEC family of enzymes with cytosine deamination activity and is primarily known for its function for generating antibody diversity and Ig class switching in B cells [8] but also implicated as a regulator of DNA demethylation [9–11]. By comparing reprogramming of wild-type and AICDA-null somatic cells, we found that AICDA is not essential but that it facilitates the efficient erasure of epigenetic memory (DNA demethylation) at a relatively late stage of reprogramming. Many isolated *Aicda*$^{-/-}$ iPSC clones fail to maintain pluripotency and they differentiate. However, with continuous passaging, up to 50% of isolated clones could be maintained and stabilized in culture. We observed hypermethylation in reprogrammed *Aicda*$^{-/-}$ cells as compared with *Aicda*$^{+/+}$ iPSCs, suggesting direct or indirect regulation of DNA demethylation by AICDA [10]. Subsequent to that initial study, two papers [12, 13] reported that iPSCs can be generated from *Aicda*$^{-/-}$ fibroblasts as efficiently as from *Aicda*$^{+/+}$ fibroblasts, prompting us to investigate technical differences in the studies that might explain the disparity. One clue was that we observed emergence of SSEA1+ cells after 3 days of transduction using lentiviral vectors, whereas Shimamoto et al. [13] reported SSEA1+ cells only after 12 days of reprogramming. In another report, Habib et al. [12] reported generation of iPSCs reprogrammed from *Aicda*$^{-/-}$ fibroblasts in a medium containing basic fibroblast growth factor (bFGF) that supports maintenance of primed PSCs. Taking these observations into account, we report here that indeed stable reprogramming can be achieved in murine cells lacking AICDA when kinetics of reprogramming is slowed, but regardless the AICDA-deficient iPSCs fail to acquire the naïve PSC state achieved by inner cell mass-derived ESCs due to failure to suppress FGF/extracellular signal-regulated kinases (ERK) signaling and remain in a partially reprogrammed state that is primed for differentiation, similar to postimplantation-derived EpiSCs.

Materials and Methods

Reprogramming

Wild-type and AICDA-mutant fibroblasts were reprogrammed using a STEMCCA lentiviral vector expressing four Yamanaka factors [14] as described [10]. Lentiviral titers were measured using QuickTiter Lentivirus Titer kit (Cell Biolabs Inc., San Diego, CA). Lenti-X qRT-PCR titration kit (Takara, Kusatsu) was used to measure viral RNA genome content. Cells were cultured in the presence of 5% CO_2 and normal oxygen conditions.

Cell Culture Media

Leukemia inhibitory factor (LIF)/serum medium—Dulbecco's modified Eagle's medium (DMEM) (Corning, New York, NY), 15% serum (Sigma, St. Louis, MO), 1,000 U LIF (Millipore, Burlington, MA), ×1 Glutamax (Life Tech.), ×1 nonessential amino acid (Invitrogen, Carlsbad, CA), 100 U/ml penicillin and 100 μg/ml streptomycin, 1 mM NA Pyruvate (Life Tech., Carlsbad, CA), and 0.1 mM 2-mercaptoethanol (Life Tech.) EpiSC medium—DMEM F12 (HyClone, Logan, UT), ×0.5 N2 (Life Technologies), ×0.5 B27 (Life Tech.), 12 ng/ml bFGF (R&D, Minneapolis, MN), 20 ng/ml ActivinA (R&D), ×1 nonessential amino acid, 50 μg/ml bovine serum albumin (BSA; Life Tech.), 0.1 mM 2-mercaptoethano, ×1 Glutamax, 100 U/ml penicillin, and 100 μg/ml streptomycin. 2i-medium—DMEM, neurobasal medium (Invitrogen), ×1 N2, ×1 B27, 0.1% BSA (Life Technologies) 100 U/ml penicillin and 100 μg/ml streptomycin supplemented with 3 μM CHIR99021, 1 μM PD03259010, 1,000 U LIF and 0.1 mM 2-mercaptoethanol, and ×1 Glutamax.

Differentiation

EBs were aggregated in LIF-free ESC media. About 5×10^5 cells were plated in 10 cm petri dishes supplemented with 10 ml medium. Medium was changed every other day. Early mesodermal differentiation was performed as described [15]. For smooth muscle differentiation, day 6 EBs were plated on gelatin-coated dishes and cultured for another 7 days in the LIF-free ESC media. Cardiomyocytes were differentiated as described [16]. Early definitive endoderm differentiation was performed as described [17]. For liver differentiation, day 6 EBs were plated onto gelatin-coated dishes in MES media lacking LIF, containing 0.5% fetal bovine serum (FBS) and 50 ng/ml activin (R&D) for 7 days. Early ectodermal differentiation was performed as described [18]. For neural differentiation, day 6 EBs were cultured in medium containing DMEM F-12 (Cellgro, Manassas, VA), 0.5% N2 (Gibco, Gaithersburg, MD), and 0.5% B27 (Gibco) supplements, 1 mM L-glutamine, 1% nonessential amino acids (Gibco), and 1.5×10^{-4} M monothioglycerol for another 3 days, after which EBs were seeded onto gelatin coated dishes with the same medium, plus 10 μM retinoic acid (Sigma) for another 4 days.

Gene Expression

Total RNA was extracted using the RNeasy Mini Kit (Qiagen, Hilden, Germany). cDNA was synthesized using a SuperScript VILO cDNA Synthesis Kit (Invitrogen). Quantitative real-time polymerase chain reaction (qRT-PCR) was performed using SYBR green Master I (Roche, Basel, Switzerland). Data were generated on a LightCycler 480 II (Roche) and analyzed using LightCycler 480 software. All quantifications were normalized to an endogenous *TBP* control. Primers used for qRT-PCR are indicated in Supporting Information Table S1.

Western Blotting

Whole-cell extracts were collected in RIPA lysis buffer (Millipore) in the presence of Protease/Phosphatase inhibitor (Cell Signaling, Danvers, MA). Proteins were resolved by electrophoresis on 10% NuPage Bis-Tris gels (Invitrogen) and transferred to poly(vinylidene difluoride) membranes (Bio-Rad, Hercules, CA). Membranes were blocked in 5% IgG-free BSA and probed overnight with antibodies. Rabbit anti-NANOG (Abcam, Cambridge, UK), goat anti-Brachyury (R&D), rabbit anti-pERK1/2 (Cell Signaling), rabbit anti-tERK1/2 (Cell Signaling), rabbit anti-tSTAT3 (Cell Signaling), rabbit anti-EED1 (Cell Signaling), rabbit anti-JARID2 (Novus Bio., Centennial, CO), rabbit anti-EZH1 (Active Motif,

Carlsbad, CA), and rabbit anti-EZH2 (Active Motif) were used. Proteins were visualized with horseradish peroxidase-conjugated secondary antibodies (Bio-Rad). Quantification was performed using Image J software.

Immunostaining and Alkaline Phosphatase Activity

Cells were fixed in tissue culture dishes with 4% paraformaldehyde (PFA) at room temperature (RT) for 20 minutes. Blocked for an hour in phosphate-buffered saline (PBS) supplemented with 10% FBS, 0.1% IgG-free BSA (Jackson ImmunoResearch, West Grove, PA) and 0.1% saponin (Sigma) at RT. Cells were incubated with primary antibody overnight at 4°C with in blocking buffer. Fluorescence-conjugated secondary antibody was used for visualization. Rabbit anti-NANOG (Abcam), rabbit anti-PAX6 (ThermoFisher, Waltham, MA), mouse anti-SMA (Abcam), rabbit anti-AFP (NeoMarkers, Fremont, CA), mouse anti-TNT (Abcam), and mouse anti-BIII-tubulin (eBiosciences, San Diego, CA) were used. Nuclei were labeled with 4′,6-diamidino-2-phenylindole (Molecular Probes, Invitrogen). Images were collected on a Zeiss epifluorescence microscope with AxioVision software. For Flow cytometry analysis cells were either fixed with 4% PFA before staining or stained alive. Staining buffer was PBS with 10% serum, and 0.1% BSA. Mouse anti-CXCR4 (eBiosciences), mouse anti-c-KIT (eBiosciences), rat anti-CD24 (BD biosciences), goat anti-Bry (R&D), and mouse anti-PDGFRα (eBiosciences) were used. Vector blue Alkaline Phosphatase Substrate Kit (Vector Laboratories, Burlingame, CA) was used to measured ALP activity following manufacturer's instructions.

Annexin V Staining

Apoptosis was detected by a PE Annexin V Apoptosis Detection Kit (BD Pharmingen, Billerica, MA) following manufacturer's instructions. Floating and attached cells were collected for apoptotic studies. Cells were run on a BD-Accuri C6 flow cytometer (BD Biosciences, Billerica, MA) and analyzed using FlowJo software.

RNA Sequencing

RNA samples were used to prepare the library with TruSeq RNA Library Prep Kit v2 (Illumina, San Diego, CA) and submitted to WCMC Genomics Core Facility for sequencing. RNA sequencing (RNA-seq) data were aligned to the GRCz10 reference genome. RNA-seq alignment and differential gene expression analysis was performed as described [19]. Raw RNA-seq data are available in the GEO public depository, accession number: GSE129223.

Enhanced Reduced Representation Bisulphite Sequencing

The WCMC Epigenomics Core Facility carried out enhanced reduced representation bisulphite sequencing (ERRBS) including alignment and methylation extraction for ERRBS data [20]. Differentially methylated regions (DMRs) were defined as regions containing at least five differentially methylated CpGs, where contiguous differentially methylated CpGs are separated by 250 bp or less, and for which the total methylation change between wild-type and *Aicda* knockout (KO) cells is 10% or more (calculated using all CpGs within the considered region including those that were not called as differentially methylated). DMR calling was performed with a script following the criteria of Pan et al. [21]. DMRs were mapped to promoters as defined by Chen et al. [22] or enhancers and super enhancers as defined by Dowen et al. [23]. Raw ERRBS data are available in the GEO public depository, accession number: GSE129223.

Statistical Analysis

Statistical analysis was performed using Excel or Prism. Significance was assessed by two-tailed, unpaired Student's *t* test and two-way analysis of variance. Heat maps were generated using R.

Results

Aicda$^{-/-}$ iPSCs Are Stable When Derived Using Relatively Low Viral Titers

We reported previously that *Aicda*$^{-/-}$ fibroblasts reprogrammed using lentiviral vectors expressing four Yamanaka factors fail to stabilize as iPSCs [10] unless at 2 weeks of reprogramming the early colonies are picked and clones continuously passaged. The function for AICDA appears to be relatively late in the process, as during the first 2 weeks of reprogramming, *Aicda*$^{-/-}$ iPSCs appeared similar to *Aicda*$^{+/+}$ iPSCs, for example, expressing early pluripotency markers, with the mutant cells failing to maintain ESC-like colony morphology and the expression of various pluripotency-associated markers such as NANOG over the next 7–14 days. Since our report, in contrast, Shimamoto et al. [13] reported equivalent reprogramming of wild-type and AICDA-mutant fibroblasts, although in both cases with low efficiency and with a significant delay in the kinetics of reprogramming. We hypothesized that the different results from the two studies could be related to the kinetics of reprogramming and tested this by using various titers of lentiviral vectors.

Lentiviral titers were calculated by measuring the levels of virus-associated capsid protein p24 (VA-p24). We compared reprogramming in the presence of serum + LIF using different concentrations of lentiviruses (Fig. 1). Fifty thousand cells were infected in each well of a 12-well plate with 500 µl of medium. One nanogram per milliliter VA-p24 corresponded to 6×10^8 RNA copies per milliliter. Indeed, we found that *Aicda*$^{-/-}$ iPSCs can be stabilized and maintain pluripotent characteristics even during the later stages of reprogramming when a lower concentration of lentiviruses was used, although as expected fewer colonies are generated. Stable ALP+ iPSC colonies were obtained from *Aicda*$^{-/-}$ tail fibroblasts when reprogramming kinetics was slowed using VA-p24 between 0.01 and 0.02 ng/ml (Fig. 1B). Wild-type fibroblasts were reprogrammed equivalently under these conditions, with increasing numbers of colonies formed in a dose-dependent manner (Fig. 1B, 1C). In contrast, additional virus leads to a loss in reprogramming for the mutant fibroblasts (Fig. 1B, 1C). When reprogrammed for 4 weeks with lower levels of virus, both wild-type and *Aicda*-mutant iPSC colonies maintain an ESC-like morphology (Fig. 1D, left and middle panels) and the expression of NANOG (Fig. 1E, left panel). In contrast, when reprogrammed using higher amounts of virus, the mutant (but not the wild type) iPSC colonies lost ESC-like morphology (Fig. 1D, right panel) as well as the expression of core pluripotency marker NANOG (Fig. 1E, right panel) and acquired more mesenchymal-like morphology. To determine if high titers of virus induce cell death, we assayed cell death by measuring the percentage of 7AAD-positive cells using flow

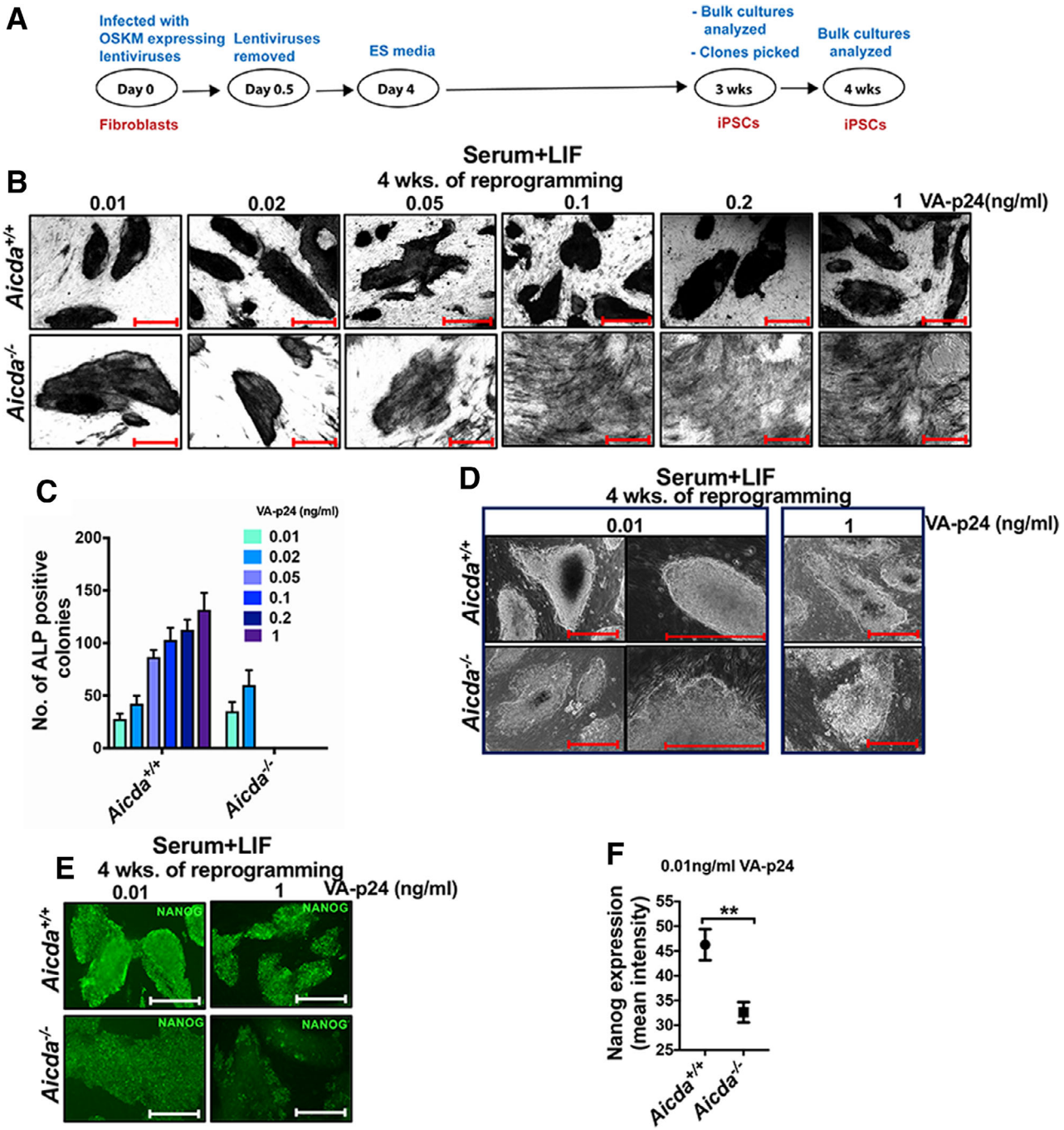

Figure 1. *Aicda*$^{-/-}$ *iPSCs* are stable only when reprogrammed using limiting titers of lentiviruses expressing Yamanaka factors. **(A):** Schematic diagram showing reprogramming strategy of fibroblasts using four Yamanaka factors. **(B):** Representative ALP activity of *Aicda*$^{+/+}$ and *Aicda*$^{-/-}$ iPSCs reprogrammed for 4 weeks using various concentrations of lentiviruses, depicted as VA-p24. Scale bar = 200 μm. See also Supporting Information Figure S1A. **(C):** Number of colonies positive for ALP activity reprogrammed for 4 weeks, $n = 3$. **(D):** Representative phase contrast images and **(E)** representative NANOG expression measured by immunochemistry in *Aicda*$^{+/+}$ and *Aicda*$^{-/-}$ iPSC colonies reprogrammed for 4 weeks using 0.01 or 1 ng/ml of VA-p24. **(F):** Mean intensity of NANOG expression in individual *Aicda*$^{+/+}$ and *Aicda*$^{-/-}$ iPSC colonies. See also Supporting Information Figure S1E. All data represented as mean ± SD. Scale bars = 500 μm. **, $p < .01$. Abbreviations: AICDA, activation-induced cytidine deaminase; iPSCs, Induced pluripotent stem cells; LIF, leukemia inhibitory factor; VA-p24, virus-associated capsid protein p-24.

cytometry. Increased viral concentration was not associated with cell death, as cells infected with high viral titers were equivalent in this assay to cells infected with low viral titers (Supporting Information Fig. S1A). With prolonged reprogramming, we observed more cell death, but no significant differences were observed between *Aicda*$^{+/+}$ and *Aicda*$^{-/-}$ cells (Supporting Information Fig. S1A). As viral supernatant may contain impurities that can affect the reprogramming process, we resuspended concentrated viruses in PBS and performed reprogramming. Viruses resuspended in PBS neither induced

cell death (Supporting Information Fig. S1B) nor altered the reprogramming process (Supporting Information Fig. S1C). Moreover, we measured the expression of lentiviral transgenes by qRT-PCR after 72 hours of infection and observed direct correlation between lentiviral dose and transgene expression. Importantly, expression levels were similar between *Aicda*$^{+/+}$ and *Aicda*$^{-/-}$ cells at all the doses (Supporting Information Fig. S1D), ruling out that the possibility that lack of AICDA affects transgene expression. Therefore, in our hands, stabilization of *Aicda*$^{-/-}$ iPSCs during reprogramming depends on the lentiviral titers used for reprogramming.

Aicda$^{-/-}$ iPSCs Derived Using Low Viral Titers Are Distinct from *Aicda*$^{+/+}$ iPSCs

Although *Aicda*$^{-/-}$ iPSCs can be stabilized using lower viral titers, the resulting colonies derived at the end of the reprogramming process appeared distinct from *Aicda*$^{+/+}$ iPSCs. Mutant iPSC colonies lacked the typical dome-shaped ESC morphology and appeared more spread out and flatter than wild-type iPSC colonies (Fig.1D, left and middle panels). Moreover, stabilized *Aicda*$^{-/-}$ iPSC colonies showed relatively lower expression levels of core pluripotency marker NANOG (Fig. 1E, left panel, 1F; Supporting Information Fig. S1E). These phenotypes suggest that although *Aicda*$^{-/-}$ iPSCs can be generated they may represent a different state of pluripotency. In the following experiments, we closely compared wild-type iPSCs with *Aicda*-mutant clones that were all generated using the relatively lower amounts of lentiviral expression vectors, in which the reprogramming kinetics and efficiency are similar and tolerated.

Aicda$^{-/-}$ iPSC colonies already appeared morphologically distinct from wild-type colonies starting from 3 weeks of reprogramming, appearing flatter and more spread (Fig. 2A, left panels; Supporting Information Fig. S2A). Likewise, even at 3 weeks, the mutant iPSCs displayed lower expression levels of NANOG than *Aicda*$^{+/+}$ iPSCs (Fig. 2A, right panels, 2B). RT-qPCR assays showed that *Aicda*$^{-/-}$ iPSCs expressed lower transcript levels for pluripotency markers compared with *Aicda*$^{+/+}$ iPSCs (Fig. 2C). We did not observe significant differences in the kinetics of reprogramming between *Aicda*$^{-/-}$ iPSCs and *Aicda*$^{+/+}$ iPSCs at early stages (Supporting Information Fig. S2B), indicating the differences observed are not due to slower reprogramming of *Aicda*$^{-/-}$ cells. Pluripotency of *Aicda*$^{-/-}$ iPSCs was evaluated by EB formation assays. Bulk cultures of iPSCs reprogrammed for 3 weeks were aggregated in the absence of LIF in serum and both *Aicda*$^{-/-}$ iPSCs and *Aicda*$^{+/+}$ iPSCs generated similar spherical EBs (Supporting Information Fig. S2C), indicating that both are functionally pluripotent.

ESCs derived from the preimplantation blastocyst are considered to represent a "naïve" state, whereas EpiSCs derived from the postimplantation epiblast represent a "primed" pluripotent state [24]. EpiSC colonies are larger and flatter than naïve PSCs colonies, which are compact and dome shaped, and the EpiSCs display lower expression levels of pluripotency markers [25]. As described above, *Aicda*$^{-/-}$ iPSCs manifest these characteristics of EpiSCs. Thus, we investigated further EpiSC-like characteristics of *Aicda*$^{-/-}$ iPSCs. Compared with ESCs, EpiSCs express higher levels of differentiation/epiblast markers including *Bry, Fgf5, Sox17, Eomes,* and *Cer1* [25]. According to RT-qPCR assays, *Aicda*$^{-/-}$ iPSCs had significantly higher expression levels for each of these genes compared with *Aicda*$^{+/+}$ iPSCs (Fig. 2D), shown also at the protein level by Western blotting analysis for BRACHYURY (Supporting Information Fig. S2D). *Aicda*$^{-/-}$ iPSCs displayed a higher percentage of CD24 positive cells, a cell surface marker identifying EpiSCs [26], compared with *Aicda*$^{+/+}$iPSCs (Fig. 2E). Thus, *Aicda*$^{-/-}$ iPSCs can be stabilized but fail to achieve the naïve pluripotent state capable by wild-type cells and appear to remain held in a state similar to EpiSCs.

Individual iPSC clones were picked after 3 weeks of reprogramming and propagated in the presence of serum + LIF. *Aicda*$^{-/-}$ iPSCs proliferated at a rate similar to *Aicda*$^{+/+}$ iPSCs (2×10^5 cells plated in a single well of a 12 well plate; Supporting Information Fig. S2E), with no differences in the cell survival as measured by Annexin V staining (Supporting Information Fig. S2F, S2G). Although the *Aicda*$^{-/-}$ iPSC clones could be propagated in the presence of serum + LIF, they were morphologically distinct from wild-type iPSCs, consistent with colonies observed during the process of reprogramming, with *Aicda*$^{-/-}$ iPSC colonies appearing flatter compared with wild-type iPSCs (Fig. 2F). RNA was harvested from iPSC clones at day 4 after passaging and qRT-PCR performed to measure transcript levels for pluripotency genes. The *Aicda*$^{-/-}$ iPSC clones, similar to bulk cultures, displayed relatively lower expression levels of pluripotency markers (Fig. 2G) and a higher frequency of CD24 positive cells (Fig. 2H). After only 4 days after passaging, we did not observe for *Aicda*$^{-/-}$ iPSCs increased expression levels of differentiation markers, perhaps due to the fact that in serum + LIF conditions, iPSCs tend to adjust their fate toward metastable PSCs [27]. However, in contrast to wild-type cells, when *Aicda*$^{-/-}$ iPSCs were plated at the same density (1×10^5 cells in a single well of a 12 well plate) and cultured without passaging to day 7, they started to differentiate from the edges of the colonies (Fig. 2I), upregulated the expression of differentiation markers (Fig. 2J), and displayed a higher percentage of BRACHYURY positive cells (Fig. 2K), demonstrating that *Aicda*$^{-/-}$ iPSC clones in serum + LIF conditions are primed for differentiation. Thus, both in bulk cultures, or as individual clones, *Aicda*$^{-/-}$ iPSCs can be stabilized but fail to achieve the naïve pluripotent state of wild-type cells and are blocked in a primed pluripotent state. In support, when iPSC clones were forced to differentiate in the absence of LIF as EBs for 5 days, *Aicda*$^{-/-}$ iPSC clones displayed higher upregulation of differentiation associated genes compared with *Aicda*$^{+/+}$ iPSC clones (Supporting Information Fig. S2H).

We also tested the propagation of wild-type or *Aicda*-mutant clones in medium permissive for maintenance and self-renewal of EpiSCs. Clones were picked after 3 weeks of reprogramming and propagated in medium containing ActivinA and bFGF [28]. Under these conditions, *Aicda*$^{-/-}$ iPSC clones maintain a more pluripotent-like colony morphology compared with *Aicda*$^{+/+}$ iPSC (Supporting Information Fig. S2I), displayed less cell death (Supporting Information Fig. S2J) and less proliferation (Supporting Information Fig. S2K), consistent with the mutant cells being maintained in a partially reprogrammed state similar to EpiSCs.

To further evaluate if the primed mutant cells are functional, we accessed the differentiation potential of *Aicda*$^{-/-}$ iPSCs by differentiating into derivatives of each of the three germ layers by performing directed differentiation assays in serum-free conditions. We measured the efficiency of differentiation toward various progenitor cells. Although in the absence of serum, during very early stages, we did not observe significant differences in the expression of lineage markers

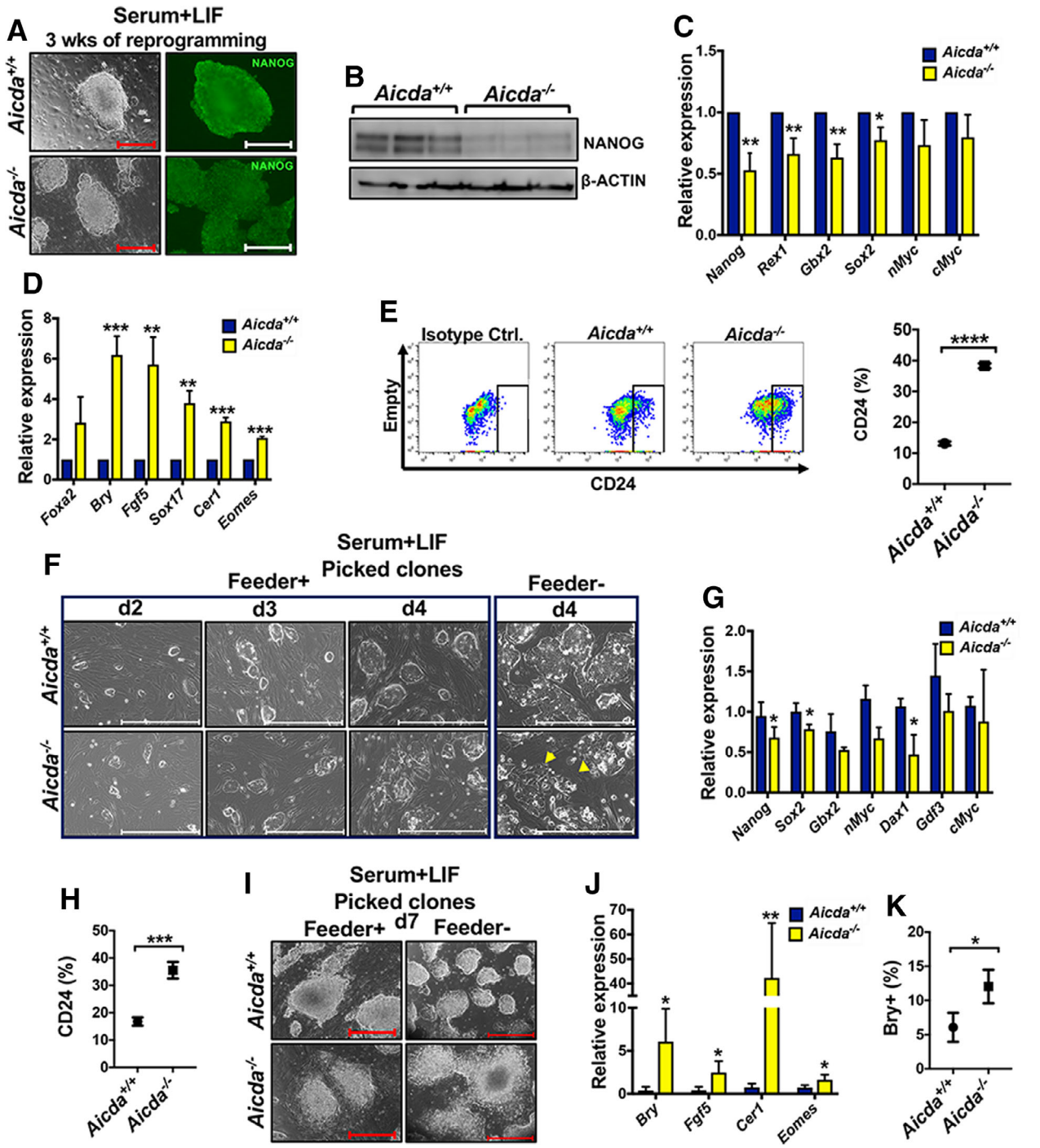

Figure 2. *Aicda* mutant induced pluripotent stem cells (iPSCs) are primed for differentiation and are similar to epiblast stem cells. **(A):** Left panel, representative phase contrast images of *Aicda*$^{+/+}$ and *Aicda*$^{-/-}$ iPSC colonies reprogrammed for 3 weeks using 0.01 ng/ml of virus-associated p-24. Right panel, representative NANOG expression of such colonies. **(B):** Western blotting analysis of NANOG expression after 3 weeks of reprogramming, representing three independent experiments. **(C):** Relative expression of pluripotency genes and **(D)** differentiation-associated genes in *Aicda*$^{-/-}$ iPSCs and *Aicda*$^{+/+}$ iPSCs reprogrammed for 3 weeks, measured by quantitative real-time polymerase chain reaction (qRT-PCR), normalized to *Aicda*$^{+/+}$ iPSCs, bulk cultures; $n = 3$. **(E):** Flow cytometry analysis of CD24 expression after 3 weeks of reprogramming, $n = 3$. **(F):** Representative phase contrast images displaying colony morphology of *Aicda*$^{+/+}$ and *Aicda*$^{-/-}$ iPSC clones cultured in serum/LIF media for 2, 3, and 4 days. Arrowheads indicate flat colonies lacking clear borders. **(G):** Relative expression of pluripotency genes measured by qRT-PCR, in *Aicda*$^{+/+}$ iPSC and *Aicda*$^{-/-}$ iPSC clones cultured for 4 days in serum/LIF media, normalized to an *Aicda*$^{+/+}$ iPSC clone; $n = 3$. **(H):** Flow cytometry analysis of CD24 expression in *Aicda*$^{+/+}$ iPSC and *Aicda*$^{-/-}$ iPSC clones cultured for 4 days in serum/LIF media, $n = 3$. **(I):** Representative colony morphology of *Aicda*$^{+/+}$ and *Aicda*$^{-/-}$ iPSC clones, cultured for 7 days in serum/LIF media. **(J):** Relative expression of genes associated with differentiation measured by qRT-PCR, data normalized to an *Aicda*$^{+/+}$ iPSC clone; $n = 4$. **(K):** Percentage of BRACHYURY positive cells measured by flow cytometry in *Aicda*$^{+/+}$ iPSC and *Aicda*$^{-/-}$ iPSC clones cultured for 7 days in serum/LIF media; $n = 3$. All data represented as mean ± SD. Scale bars = 500 μm. *, $p < .05$; **, $p < .01$; ***, $p < .001$; ****, $p < .0001$. Abbreviations: AICDA, activation-induced cytidine deaminase; LIF, leukemia inhibitory factor.

between mutant and wild-type cells (Supporting Information Fig. S3A, S3E, S3H), we observed that *Aicda*$^{-/-}$ iPSCs differentiated more efficiently into mesodermal progenitors (PDGRFα+) than endodermal progenitors (CXCR4/c-KIT+; Supporting Information Fig. S3B, S3F, respectively). This suggests that in the absence of AICDA, reprogrammed iPSCs may retain the epigenetic memory of parent fibroblasts, which are of mesodermal origin. However, we did not observe significant differences in the capacity to differentiate into ectodermal progenitors (Supporting Information Fig. S3I). Like *Aicda*$^{+/+}$ iPSCs, *Aicda*$^{-/-}$ iPSCs can differentiate into smooth muscle cells (Supporting Information Fig. S3C), cardiomyocytes (Supporting Information Fig. S3D), hepatocytes (Supporting Information Fig. S3G), and neurons (Supporting Information Fig. S3J), indicating that *Aicda*$^{-/-}$ iPSCs are pluripotent and functional.

Aicda$^{-/-}$ iPSC Clones Have Suppressed Expression of Mitogen-Activated Protein Kinase Signaling Pathway Inhibitors

To further investigate the role of AICDA in facilitating naive pluripotency, global transcriptional profiles were analyzed in both *Aicda*$^{+/+}$ iPSC clones and *Aicda*$^{-/-}$ iPSC clones by RNA-seq. Clones were picked after 3 weeks of reprogramming and passaged at least 3 times to expand cells for RNA extraction. The reprogramming process is associated with genetic instability, and in addition, AICDA is a mutagen that is known for its effect on genetic stability [29, 30]. Therefore, before performing RNA-seq analysis, the cells were profiled by G-band karyotyping, with a goal to analyze karyotypically normal iPSC clones. Surprisingly, we found that *Aicda*$^{-/-}$ iPSC clones are genetically more unstable than *Aicda*$^{+/+}$ iPSC clones, consistent with the fact that murine primed stem cells develop karyotypic abnormalities more frequently compared with ground state stem cells [31]. In several attempts, we failed to obtain primarily karyotypically normal *Aicda*$^{-/-}$ clones from a single reprogramming experiment, in contrast to mostly normal karyotypes obtained with wild-type cells. Therefore, we performed RNA-seq analysis on three *Aicda*$^{-/-}$ iPSC clones including one with normal karyotype and two with relatively minor chromosomal abnormalities, and compared with three wild-type clones that were karyotypically normal (Supporting Information Fig. S4A). Although some deregulated genes might be missed due to the abnormalities, the subsequent analysis focused on changes that were consistent across all clones, and therefore, are independent of an abnormal karyotype.

RNA-seq analysis identified approximately 500 differentially regulated genes comparing *Aicda*$^{-/-}$ and *Aicda*$^{+/+}$ iPSC clones (log2 fold change, greater than 2 or less than −2, adjusted p value < .05). Two hundred forty-seven genes were upregulated and 282 genes downregulated in *Aicda*$^{-/-}$ iPSC clones compared with *Aicda*$^{+/+}$ iPSC clones (Fig. 3A). Despite two mutant clones displaying minor chromosomal abnormalities, unsupervised hierarchical clustering analysis at either the global level or focused on the top 1,000 upregulated and downregulated genes, correctly grouped the wild-type and mutant clones (Supporting Information Fig. S4B and Fig. 3B, respectively), implying that chromosomal abnormalities did not have a significant impact on global gene expression. The RNA-seq analysis confirmed downregulation of known pluripotency genes in *Aicda*$^{-/-}$ iPSCs compared with *Aicda*$^{+/+}$ iPSCs (Fig. 3C). Intriguingly, gene ontology analysis of biological processes using the top 200 downregulated genes in *Aicda*$^{-/-}$ iPSCs displayed enrichment for genes involved in metabolic processes and the mitogen-activated protein kinase (MAPK) signaling pathway, the signaling pathway known to be a master regulator of the pluripotency network (Fig. 3D). The MAPK signaling pathway plays a critical role in balancing pluripotency versus differentiation in ESCs. Suppression of MAPK signaling directs mouse ESCs (mESCs) toward a naïve pluripotent state, whereas activation is required for cells to exit from pluripotency [32]. Notably, we found that MAPK signaling related genes that are downregulated in *Aicda*$^{-/-}$ iPSCs include genes encoding negative regulators of MAPK signaling such as Sproutys (Sprys) and Dual-specificity protein phosphatases (DUSPs) [33] (Fig. 3E). Sprouty and DUSP proteins are key regulators of MAPK signaling in mESCs and reduction in their levels is associated with differentiation, and high expression levels associated with stemness [34–37]. We compared the transcriptome of *Aicda*$^{-/-}$ iPSC and *Aicda*$^{+/+}$ iPSC with publicly available RNA-seq datasets of ESCs and EpiSCs [38, 39]. Unsupervised hierarchal clustering revealed that despite the fact that *Aicda*$^{-/-}$ iPSCs and EpiSCs were cultured in different media, they clustered together on the basis of defined genesets (Supporting Information Fig. S4C). Consistently, EpiSCs displayed lower expression levels of negative regulators of MAPK signaling than ESCs (Fig. 3F). Altogether, global transcriptome analysis indicated that *Aicda*$^{-/-}$ iPSC may fail to achieve a naïve pluripotent state due to a limited ability to suppress MAPK signaling.

Aicda$^{-/-}$ iPSC Have Hyperactive FGF/ERK Signaling

The ERK1/2 are MAPK members that play a pivotal role in balancing self-renewal and differentiation of mESCs [32]. The ERK signal transduction cascade mediates the effect of growth factors by sequential activation of RAS-like GTPase, RAF kinase, serine/threonine protein kinase MEK, and finally ERK [40]. Inhibition of MEK/ERK signaling by pharmacological MEK inhibitors promotes self-renewal and pluripotency of mESCs in the naïve state [41]. Based on the transcript profiling, we hypothesized that the primed state of *Aicda*$^{-/-}$ iPSCs is due to the loss of MAPK inhibitors leading to hyperactive MAPK signaling, and therefore investigated activation of ERK1/2 (pERK1/2) by Western blotting analysis. Surprisingly, we observed lower levels of pERK1/2 in lysates from *Aicda*$^{-/-}$ iPSC clones compared with *Aicda*$^{+/+}$ iPSC clones (Fig. 4A). This seemed counter-intuitive to the fact that *Aicda*$^{-/-}$ iPSCs are primed for differentiation and that activation of ERK initiates differentiation of mESCs [32]. However, it is known that in mESCs a compensatory feedback mechanism exists due to downregulation of downstream components of the MAPK pathway and that lower levels of pERK in mESCs can be indicative of hyperactive ERK signaling [36, 42]. We also investigated phosphorylation/activation of the upstream activator kinases of ERK1/2, namely MEK1/2, and observed that consistent with levels of pERK1/2, *Aicda*$^{-/-}$ iPSCs at steady state have lower levels of pMEK1/2 (Fig. 4B). Therefore, we considered that if AICDA normally suppresses the ERK signaling pathway, for example, through DUSP and Sprouty expression, the loss of this brake leads to a compensatory program that reduces steady-state levels of pMEK/pERK proteins.

To test directly hyperactive FGF/ERK signaling in *Aicda*$^{-/-}$ iPSC clones, the response of *Aicda*$^{+/+}$ and *Aicda*$^{-/-}$ iPSC clones was compared when provided with an FGF2 stimulus. The iPSC

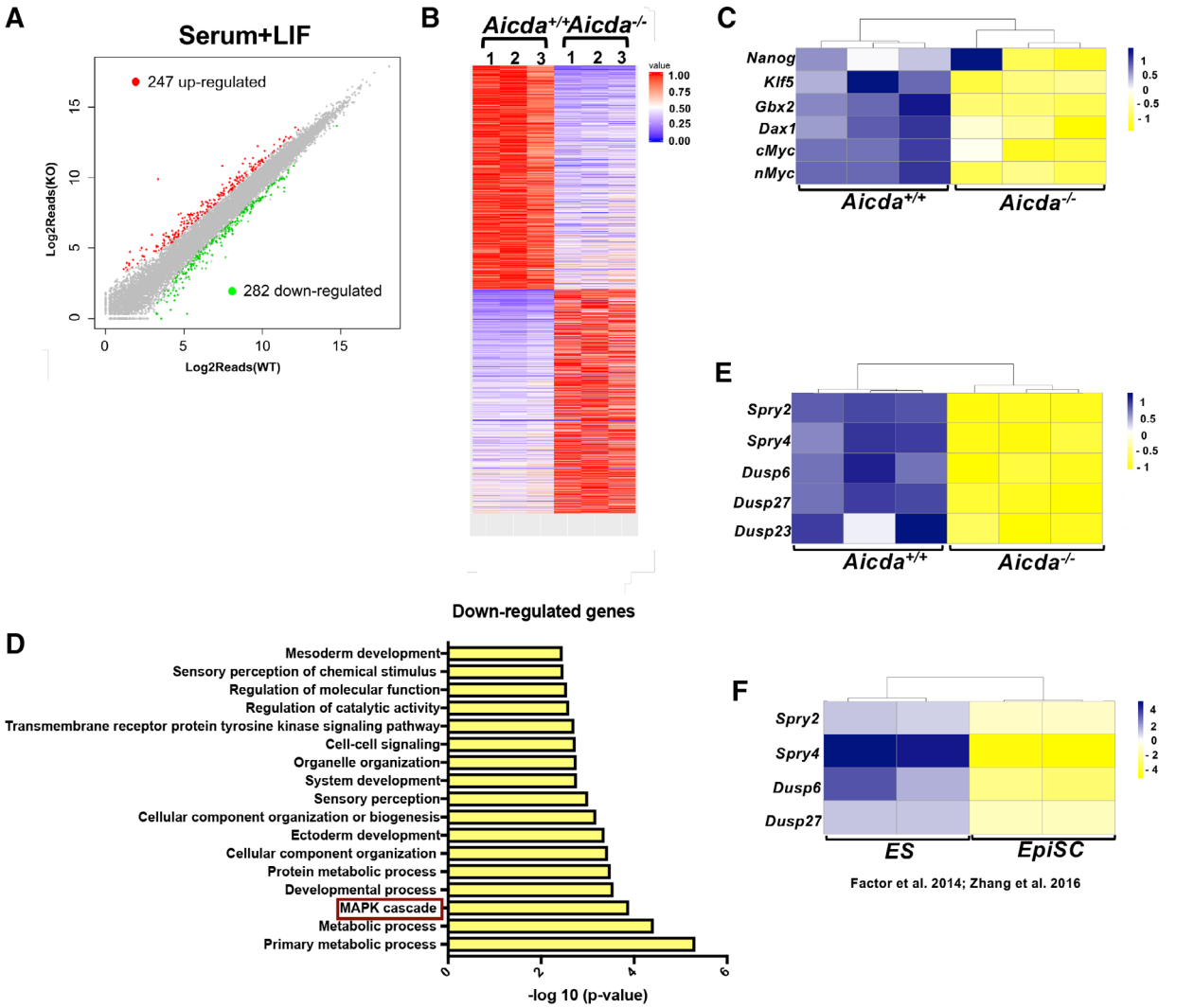

Figure 3. RNA-seq analysis of *Aicda*$^{+/+}$ and *Aicda*$^{-/-}$ induced pluripotent stem cell (iPSC) clones suggests hyperactive fibroblast growth factor/extracellular signal-regulated kinases (FGF/ERK) signaling in *Aicda*$^{-/-}$ iPSCs. **(A):** Scatter plot displaying upregulated and downregulated genes in *Aicda*$^{-/-}$ iPSC clones as compared with *Aicda*$^{+/+}$ iPSC clones. **(B):** Hierarchical clustering of 1,000 upregulated and 1,000 downregulated genes in *Aicda*$^{-/-}$ iPSC clones compared with *Aicda*$^{+/+}$ iPSC clones. See also Supporting Information Figure S4B. **(C):** Heat map displaying downregulation of transcript levels for pluripotency genes in *Aicda*$^{-/-}$ iPSC clones compared with *Aicda*$^{+/+}$ iPSC clones. **(D):** PANTHER GO-Slim biological process analysis of top 200 downregulated genes in *Aicda*$^{-/-}$ iPSC clones. **(E):** Heat map displaying downregulation of transcripts levels of negative regulators of FGF/ERK signaling in *Aicda*$^{-/-}$ iPSC clones compared with *Aicda*$^{+/+}$ iPSC clones and **(F)** in EpiSCs compared with ESCs. See also Supporting Information Figure S4C. Abbreviations: AICDA, activation-induced cytidine deaminase; EpiSC, epiblast stem cells; KO, knockout; LIF, leukemia inhibitory factor; WT, wild type.

clones were cultured in serum-free conditions in the presence of LIF for 12 hours and then stimulated with 10 ng/ml FGF2. The *Aicda*$^{-/-}$ iPSCs exhibited stronger activation of ERK signaling compared with *Aicda*$^{+/+}$ iPSCs after 5 minutes, consistent with hyperactive FGF/ERK signaling (Fig. 4C). Additionally, *Aicda*$^{-/-}$ iPSCs displayed higher expression of some of the targets of ERK signaling compared with *Aicda*$^{+/+}$ iPSCs (Fig. 4D). Moreover, *Aicda*$^{-/-}$ iPSC clones propagated better than *Aicda*$^{+/+}$ iPSC clones when cultured for two passages in the presence of 10 ng/ml FGF2 and KOSR medium (20%; Fig. 4E), supporting their primed state. Moreover, in these conditions, *Aicda*$^{-/-}$ iPSC clones displayed significantly higher levels of pERK1/2 compared with *Aicda*$^{+/+}$ iPSCs (Fig. 4F), displaying the hyperactive ERK signaling that is suppressed at steady state when the cells are grown in serum + LIF.

Treatment of *Aicda*$^{-/-}$ iPSCs with Pharmacological Inhibitors of the FGF/ERK Signaling Pathway Rescues AICDA Deficiency

Naïve PSCs rely on defined growth factor signaling pathways for maintaining pluripotency and self-renewal. For mESCs, ground state/naïve pluripotency can be established in the presence of a MAPK inhibitor [41]. In contrast, mESCs cultured in the presence of serum and LIF (serum + LIF), although capable of naïve pluripotency, are highly heterogeneous with respect to gene expression and are considered to be in a dynamic metastable state comprising two interchangeable populations corresponding to naive and primed states [27]. As *Aicda*$^{-/-}$ iPSCs cultured in serum/LIF are in a primed state with hyperactive ERK signaling, we tested if MAPK inhibition by small molecules could overcome the impact of AICDA deficiency.

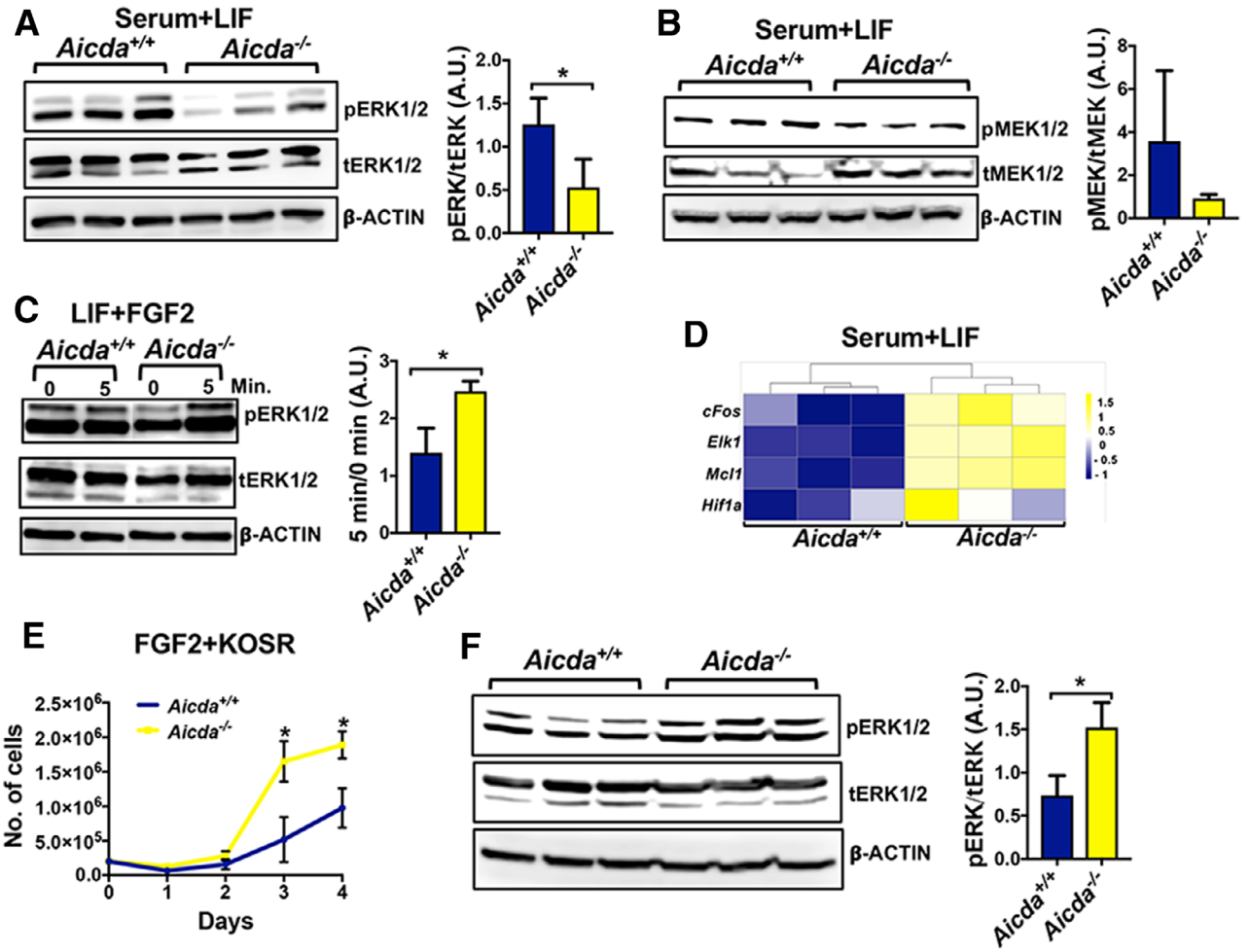

Figure 4. *Aicda*$^{-/-}$ induced pluripotent stem cell (iPSC) clones have hyperactive FGF/ERK signaling. **(A):** Western blotting analysis of pERK1/2 and tERK1/2 and **(B)** pMEK and tMEK for *Aicda*$^{-/-}$ and *Acida*$^{+/+}$ iPSC clones cultured in serum+LIF media. **(C):** Western blotting analysis of pERK1/2 and tERK1/2 after FGF2 (10 ng/ml) treatment. **(D):** Heat map displaying upregulation of transcript levels of MAPK target genes in *Aicda*$^{-/-}$ iPSC clones compared with *Aicda*$^{+/+}$ iPSC clones. **(E):** Live cell counts and **(F)** Western blotting analysis of pERK1/2 and tERK1/2 for *Aicda*$^{-/-}$ and *Acida*$^{+/+}$ iPSC clones cultured in the presence of FGF2 (10 ng/ml) for two passages. All data are represented as mean ± SD. *, $p < .05$. Abbreviations: AICDA, activation-induced cytidine deaminase; A.U., arbitrary units; ERK, extracellular signal-regulated kinases; FGF, fibroblast growth factor; LIF, leukemia inhibitory factor.

Wild-type and mutant iPSC clones were treated with either of two small molecule inhibitors of the FGF/ERK signaling pathway in the presence of serum/LIF. PD173074 is an inhibitor of the FGF receptor, whereas PD325901 functions relatively downstream as an inhibitor of MEK activation (Fig. 5A). Equal cell numbers representing AICDA-mutant or wild-type iPSCs (three independent clones) were treated with 1 μM of either small molecule inhibitor for two passages in serum/LIF medium. Treatment of *Aicda*$^{-/-}$ iPSCs with either inhibitor preserved the pluripotent state and inhibited differentiation, as observed by colony morphology (Fig. 5B). RT-qPCR results further demonstrated that inhibitor-treated *Aicda*$^{-/-}$ iPSC cells failed to differentiate when cultured for 6 days without passaging, whereas similarly cultured untreated cells upregulated the expression of differentiation associated genes (Fig. 5C).

Moreover, we tested if *Aicda*$^{-/-}$ iPSCs can achieve homogenous ground state pluripotency in a serum-free medium containing 2i, media defined for the propagation of mESCs in naïve state [41]. Three independent mutant and wild-type clones were isolated after 3 weeks of reprogramming, expanded on feeder cells for 4 days in serum/LIF conditions and then transferred to 2i medium in LIF/feeder-free conditions. Strikingly, when placed into 2i conditions the AICDA-deficient iPSCs do not survive (Fig. 5D). After two passages in 2i medium, significantly fewer cells were harvested from *Aicda*$^{-/-}$ iPSC cultures than initially plated on day 0, whereas under the same 2i conditions, the wild-type cells expanded (Fig. 5E). Accounting for this loss, we observed higher rates of early apoptotic and late apoptotic/dead cells in 2i conditions among AICDA-mutant cells compared with wild-type cells as measured by AnnexinV staining (Fig. 5F). Thus, consistent with a need for AICDA in establishment and maintenance of naïve pluripotency, AICDA-null cells fail to survive in 2i conditions that specifically support the naïve state.

Another alternative for propagating mESCs in a naïve pluripotent state for multiple passages is to culture in 2i conditions in the presence of LIF. Therefore, we cultured three independent AICDA mutant or wild-type iPSC clones in the presence of 2i + LIF and discovered that *Aicda*$^{-/-}$ iPSC clones are stable in these conditions. Similar to wild-type cells, they acquire dome-shaped colony morphology and were homogenous for expression of Nanog, features of naïve pluripotent

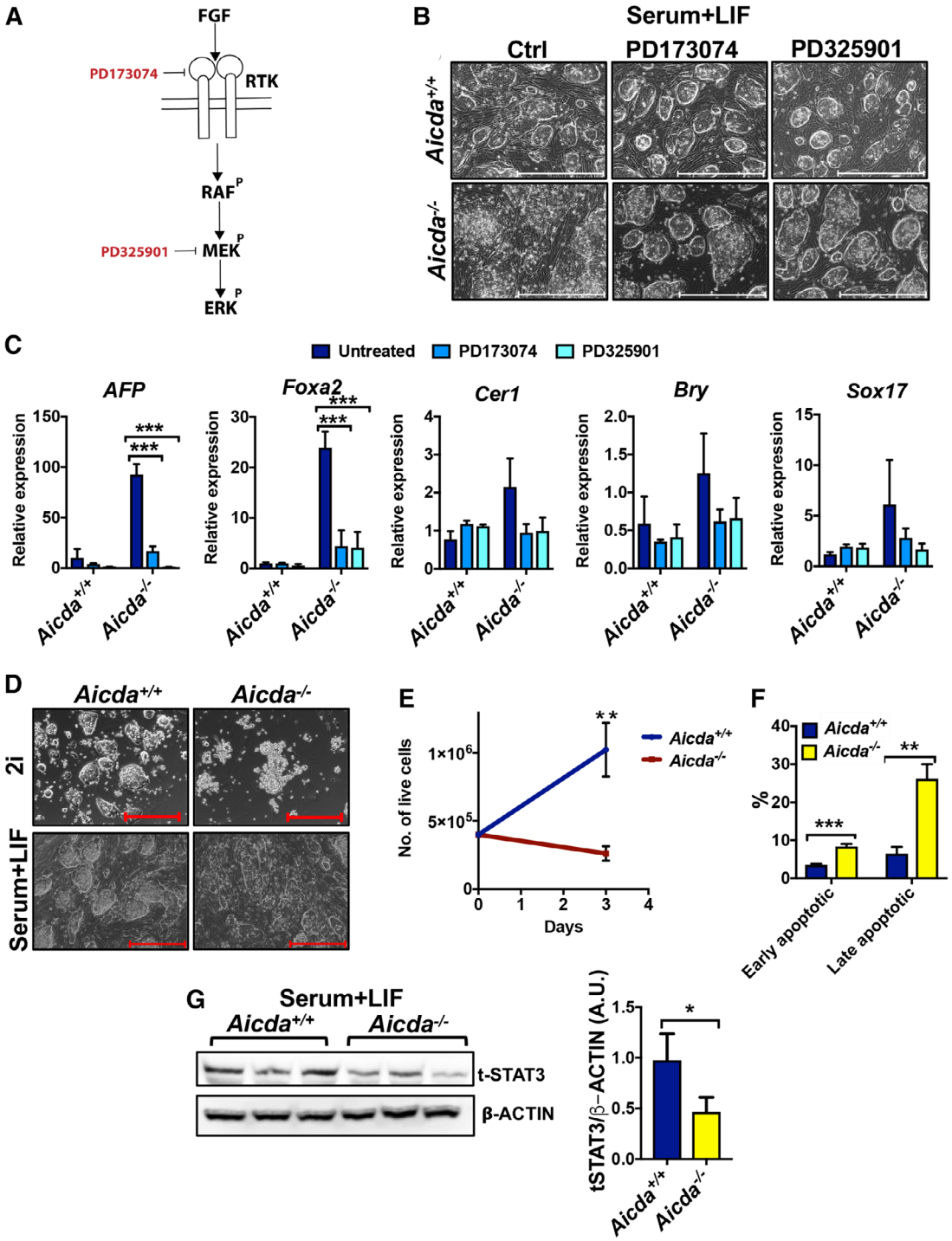

Figure 5. Treatment of *Aicda*$^{-/-}$ induced pluripotent stem cell (iPSC) clones with pharmacological inhibitors of FGF/ERK signaling prevents differentiation. **(A):** Schematic representation of FGF/ERK signaling pathway. **(B):** Representative phase contrast images of *Aicda*$^{+/+}$ and *Aicda*$^{-/-}$ iPSC clones, cultured in the presence of pharmacological inhibitors of FGF/ERK signaling for two passages. **(C):** Relative expression of genes associated with differentiation measured by quantitative real-time polymerase chain reaction, in *Aicda*$^{+/+}$ and *Aicda*$^{-/-}$ iPSC clones cultured in the presence of pharmacological inhibitors of FGF/ERK signaling for two passages, normalized to an *Aicda*$^{+/+}$ iPSC clone (n = 3). **(D):** Representative colony morphology of *Aicda*$^{+/+}$ and *Aicda*$^{-/-}$ iPSC clones cultured in 2i medium and serum/LIF for 3 days. **(E):** Live cell counts after culturing iPSC clones in 2i medium for 3 days, n = 3. **(F):** Percentage of early apoptotic and late apoptotic/dead cells measured after culturing iPSC clones in 2i medium for 3 days, n = 3. See also Supporting Information Figure S2E. **(G):** Western blotting analysis of t-STAT3 for *Acida*$^{-/-}$ and *Aicda*$^{+/+}$ iPSC clones cultured in serum/LIF media. All data represented as mean ± SD. All scale bars = 500 μm. *, $p < .05$; **, $p < .01$; ***, $p < .001$. Abbreviations: AICDA, activation-induced cytidine deaminase; A.U., arbitrary units; ERK, extracellular signal-regulated kinases; FGF, fibroblast growth factor; LIF, leukemia inhibitory factor.

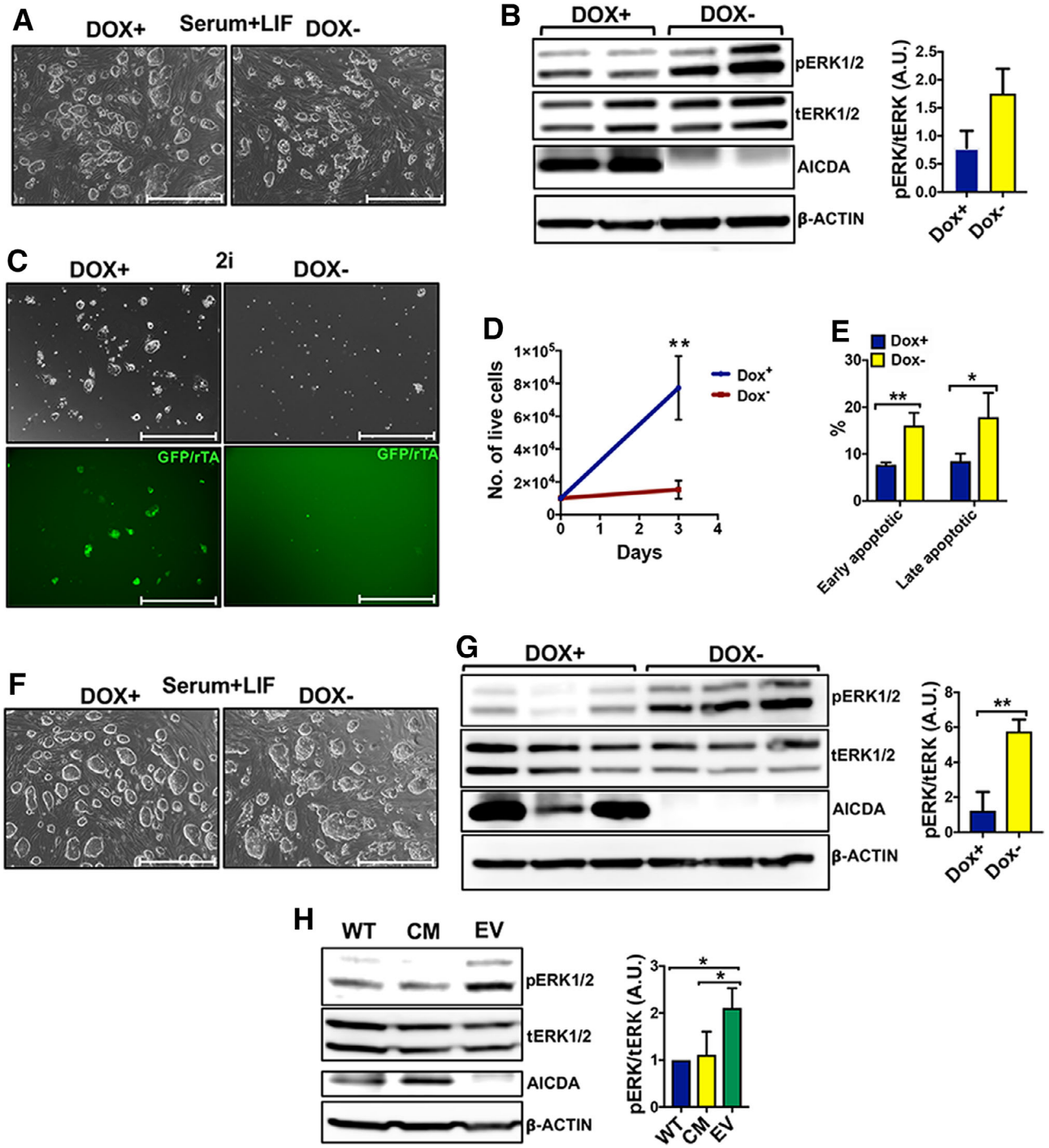

Figure 6. AICDA expression lowers the levels of pERK1/2. **(A):** Representative phase contrast images of *Aicda*$^{-/-}$ induced pluripotent stem cell (iPSC) clones infected with dox-inducible lentiviruses expressing AICDA. **(B):** Western blotting analysis of pERK1/2, tERK1/2, and AICDA for the same clones. **(C):** Representative phase contrast images (upper panel) and images displaying GFP expression (reverse tet-transactivator) (lower panel), **(D)** live cell counts, and **(E)** percentage of early apoptotic and late apoptotic/dead cells measured after culturing iPSC clones in 2i medium for 3 days. *n* = 3. **(F):** Representative phase contrast images of *Aicda*$^{+/+}$ iPSC clones infected with dox-inducible lentiviruses expressing AICDA. **(G):** Western blotting analysis of pERK1/2, tERK1/2 and AICDA for the same clones. **(H):** Western blotting analysis of pERK1/2, tERK1/2, and AICDA for *Aicda*$^{-/-}$ iPSC clones infected with retroviruses expressing AICDA (WT), CM form of AICDA, and EV. See also Supporting Information Figure S6. All data represented as mean ± SD. All scale bars = 500 μm. *, $p < .05$; **, $p < .01$. Abbreviations: AICDA, activation-induced cytidine deaminase; A.U., arbitrary units; CM, catalytically mutated; ERK, extracellular signal-regulated kinases; EV, empty vector; FGF, fibroblast growth factor; LIF, leukemia inhibitory factor; WT, wild type.

cells (Supporting Information Fig. S5A). In the presence of 2i + LIF, the *Aicda*$^{-/-}$ iPSCs maintained the expression levels of pluripotency genes, as well as wild-type cells (Supporting Information Fig. S5B). The cytokine LIF sustains self-renewal of mESCs by activating transcription factor STAT3 [43], and STAT3 activation is known to be a limiting factor for reprogramming to ground state pluripotency [44]. Therefore, we compared STAT3 expression levels between *Aicda*$^{-/-}$ iPCS and

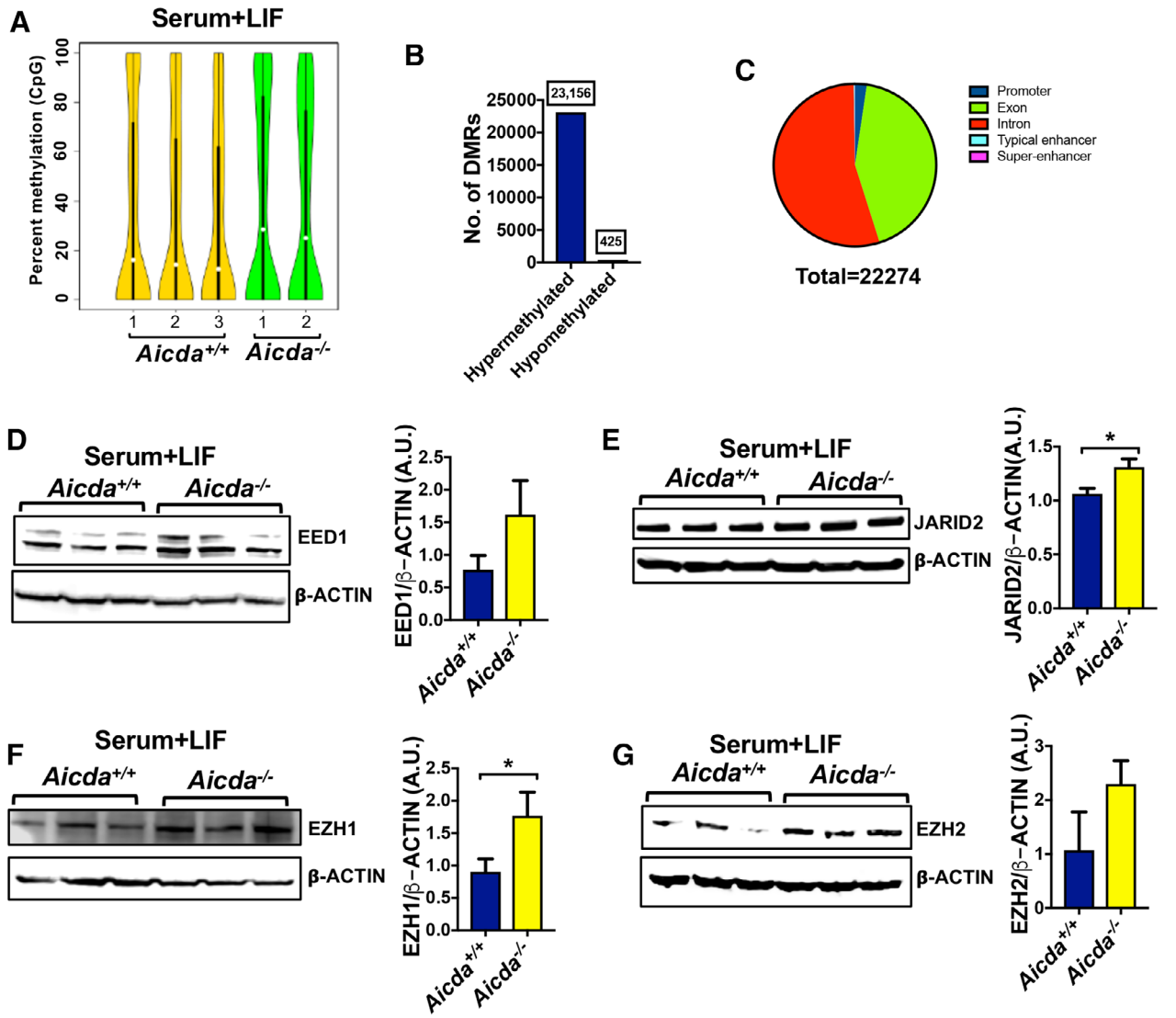

Figure 7. *Aicda*$^{-/-}$ induced pluripotent stem cells (iPSCs) are hypermethylated. **(A):** Global CpG methylation in *Aicda*$^{+/+}$ and *Aicda*$^{-/-}$ iPSC clones. **(B):** Hypermethylated and hypomethylated DMRs in *Aicda*$^{-/-}$ iPSC. **(C):** A pie chart displaying number of hypermethylated DMRs in *Aicda*$^{-/-}$ iPSC clones at different genomic regions. Western blotting analysis of EED1 **(D)**, JARID2 **(E)**, EZH1 **(F)**, and EZH2 **(G)** in *Acida*$^{-/-}$ and *Aicda*$^{+/+}$ iPSC clones cultured in serum/LIF media. All data represented as mean ± SD. *, $p < .05$. Abbreviations: AICDA, activation-induced cytidine deaminase; A.U., arbitrary units; LIF, leukemia inhibitory factor.

Aicda$^{+/+}$ iPSC clones by Western blotting and indeed observed that when cultured in serum/LIF media *Aicda*$^{-/-}$ iPCS has significantly lower levels of total STAT3 (t-STAT3; Fig. 5G), although t-STAT3 levels were variable among iPSC clones, likely attributed to clonal variation among iPSC lines [45]. Therefore, it appears that *Aicda*$^{-/-}$ iPCSs have diminished LIF-STAT3 signaling which limits their capacity to survive and be propagated in 2i conditions lacking LIF, unlike wild-type cells.

AICDA Expression Reduces pERK Levels in *Aicda*$^{-/-}$ iPSC Clones

We tested if expressing AICDA in *Aicda*$^{-/-}$ iPSC has any effect on the levels of pERK. AICDA was expressed conditionally in *Aicda*$^{-/-}$ iPSC clones using doxycycline (dox)-inducible lentiviruses [46], using a vector in which the reverse tet-transactivator and green fluorescent protein (GFP) are expressed ubiquitously under control of the *Ubc* promoter, and AICDA expression is induced by addition of dox to the culture (CS-TRE-AID-PRE-Ubc-tTA-I2G). *Aicda*$^{-/-}$ iPSC clones were infected with lentiviruses in feeder-free conditions and cells were moved back to feeders 24 hours after the infection. GFP-positive cells were sorted and divided into two wells; one well was treated with dox (dox+) to induce AICDA and the other served as control (dox–). Interestingly, dox-treated *Aicda*$^{-/-}$ iPSC clones displayed more compact morphology with sharper edges as with untreated cells (Fig. 6A; Supporting Information Fig. S6A), with lower pERK1/2 levels in dox-treated clones than untreated cells (Fig. 6B). Furthermore, we cultured iPSCs in the presence of 2i (no LIF) and observed that expression of AICDA in AICDA-null iPSCs significantly enhanced cell survival as shown by the presence of pluripotent colonies (Fig. 6C), cell number (Fig. 6D), and percent of apoptotic cells (Fig. 6E). Moreover, expression of AICDA in AICDA-null iPSCs resulted in the increased expression levels of negative regulators of FGF/ERK signaling (Supporting Information Fig. S6B).

We tested if forced expression of AICDA in wild-type cells has any impact on the levels of pERK1/2 and observed that dox-induced wild-type cells displayed more naïve PSC-like morphology than untreated cells (Fig. 6F; Supporting Information Fig. S6C). Similar to mutant cells, dox+ *Aicda*$^{+/+}$ iPSC clones displayed lower levels of pERK1/2 as compared with dox– cells (Fig. 6G), consistent with AICDA as a regulator of FGF signaling that promotes iPSCs toward the naïve state.

It was reported previously that DNA demethylation activity of AICDA can function independent of its deaminase activity [11]. Therefore, we tested if regulation of ERK signaling by AICDA depends on its deaminase activity. The *Aicda*$^{-/-}$ iPSC clones were transduced with retrovirus vectors expressing wild-type AICDA (WT), a catalytically mutated form of AICDA lacking deaminase activity (CM), or empty vector. The vectors expressed GFP [10], and GFP-positive cells were sorted after infection and passaged once before performing Western blotting analysis for pERK1/2. Intriguingly, both the wild-type and catalytically mutated forms of AICDA were able to reduce pERK1/2 levels in *Aicda*$^{-/-}$ iPSC clones (Fig. 6H; Supporting Information Fig. S6D, S6E) as well as in *Aicda*$^{+/+}$ iPSC clones (Supporting Information Fig. S6F), suggesting that regulation of pERK levels by AICDA can function independent of its deaminase activity.

Aicda$^{-/-}$ iPSC Clones Are Hypermethylated Compared with *Aicda*$^{+/+}$ iPSCs and Exhibit a Gain in Expression Levels for PRC2 Components

Previous publications reported a role for AICDA in DNA demethylation for progression of reprogramming or cancer [10, 11, 47]. When reprogramming is performed with high titer lentivirus, the absence of AICDA results in hypermethylation and limits pluripotency stabilization [10]. As the current study used low viral titers and kinetics that can be tolerated by mutant cells, we re-evaluated CpG methylation patterns under these conditions. Using ERRBS, we found that *Aicda*$^{-/-}$ iPSC DNA was globally hypermethylated compared with *Aicda*$^{+/+}$ iPSC clones (Fig. 7A). We focused on DMRs, defined as contiguous differentially methylated CpGs separated by 250 bp or less, and for which the total methylation change between wild-type and *Aicda* mutant cells is 10% or more, calculated using all CpGs within the considered region including those that were not called as differentially methylated. We observed a total of 23,581 DMRs, out of which 23,156 were hypermethylated and only 425 were hypomethylated in *Aicda*$^{-/-}$ iPSCs compared with *Aicda*$^{+/+}$ iPSC clones (Fig. 7B) reinforcing that AICDA is involved in the process of DNA demethylation. Furthermore, hypermethylated regions were highly enriched for exons and introns (Fig. 7C), corroborating the fact that AICDA-regulated methylation is less involved in regulating epigenetics of enhancers and super enhancers [11].

To gain insight into the regulation of naïve pluripotency by AICDA, we focused on PRC2 complex proteins. Reinberg's group [48] demonstrated that ERK signaling modulates chromatin features and active ERK signaling promotes increased PRC2 occupancy at developmental genes, facilitating the primed/poised status of mESCs. In the absence of ERK, developmental promoters assume a more "inert" chromatin state, facilitating naïve state. Interestingly, we observed higher levels of PRC2 complex proteins, including EED-1, JARID2, EZH1, and EZH2, in *Aicda*$^{-/-}$ iPSC clones compared with *Aicda*$^{+/+}$ iPSC clones (Fig. 7D–7G). This suggests that AICDA may facilitate a naïve pluripotent state by maintaining the chromatin in a more "inert" state through regulating PCR2 complex recruitment to developmental genes, which could be dependent or independent of DNA demethylation.

Discussion

The results presented here show that although iPSCs deficient in AICDA can be derived, they are distinct from wild-type iPSCs. They have distinct morphology, express relatively lower levels of pluripotency genes, are primed for differentiation, fail to survive in naïve pluripotency 2i culture conditions, and have better survival in primed culture conditions.

In contrast to our previous studies using high concentrations of lentiviral vectors, we were able to derive with similar efficiency wild-type or AICDA-deficient iPSCs by reprogramming using relatively low amounts of lentiviral vectors expressing four Yamanaka factors. The molecular basis for why limiting expression of pluripotency factors facilitates iPSC stabilization is unclear. However, it has been shown by Nagy and colleagues [26, 49] that higher transgene expression during reprogramming results in impaired DNA demethylation during the later stages of reprogramming, which we speculate would be further exacerbated in the absence of AICDA, leading to destabilization of *Aicda*$^{-/-}$ iPSCs. With limiting levels of factors, the kinetics of reprogramming are also slower, perhaps providing cells more time to remove epigenetic marks by other mechanisms, including passive demethylation during proliferation. Slower kinetics might also explain why a previous report [13] described stabilized *Aicda*$^{-/-}$ iPSCs, as reprogramming was significantly slower in that study with SSEA1+ cells observed only after 12 days instead of the typical 4 days using high viral titers. Regardless, here we showed that even if they are stabilized, the mutant cells are not normal and the genome remains hypermethylated. The mutant cells display distinct morphological features, lower expression of pluripotency-associated genes, higher expression of differentiation markers, and differential growth requirements [50].

FGF/ERK signaling is a master regulator of ESC pluripotency [32]. Suppression of FGF/ERK signaling promotes self-renewal of mESCs as naïve PSCs [41]. Conversely, EpiSCs require FGF signaling for maintenance and derivation. Thus, FGF/ERK signaling is a key factor directing PSCs toward various fates, suppression leading to naïve state, whereas activation drives stem cells toward a primed state [24]. Interestingly, we observed that AICDA-deficient iPSCs have hyperactive FGF/ERK signaling compared with the wild-type iPSCs, despite lower steady-state pERK levels when cultured in serum + LIF, consistent with action of negative feedback mechanisms due to upregulation of downstream targets [42]. This may explain why Von Meyenn et al. [51] observed no requirement for AICDA in achieving naive pluripotent state, as they cultured cells in the presence of a MAPK pathway inhibitor [51]; indeed we found that inhibition of MAPK signaling directs AICDA-null iPSCs to a stage similar to WT iPSCs, but only in the presence of LIF. RNA-seq profiling revealed that *Aicda*$^{-/-}$ iPSCs have strikingly lower transcript levels of negative regulators of FGF/ERK signaling including Sprouty2/4 and several DUSPs. When AICDA is forcibly expressed in either AICDA-null or wild-type iPSCs the levels of pERK are reduced, indicating AICDA suppresses pERK amidst a complex system of feedback. Nevertheless, expression of AICDA in *Aicda*$^{-/-}$ iPSCs enhanced survival in 2i medium. Furthermore, *Aicda*$^{-/-}$ iPSCs

were relatively more stable than wild-type iPSCs in medium supplemented with FGF2, and this likely accounts for the reported stable generation of *Aicda*$^{-/-}$ iPSCs [12], as that study used reprogramming culture conditions that support self-renewal of primed PSCs.

How AICDA regulates FGF/ERK signaling is unclear. AICDA is known for its function in DNA methylation either through its own deaminase activity or by regulating the function of DNMTs [11]. Quite intriguingly, we observed that AICDA-dependent modulation of pERK levels in iPSCs is independent of its deaminase activity. Although the genome remains hypermethylated and expression of AICDA in mutant cells resulted in upregulation of Sprouty2/4 and DUSP6, we could not find DMRs associated with the Sprouty/DUSP promoters. This negative result does not rule out direct modulation of these target genes but suggests that the impact on expression may be indirect or independent of methylation roles. Likewise, a direct link to how AICDA regulates STAT3 levels remains unknown. There may be a combination of AICDA targets for demethylation in addition to deaminase-independent functions of AICDA, which clearly requires further investigation.

Genomic stability is one of the hallmarks of pluripotent PSCs [52]. ESCs possess a distinctive caretaking network to maintain genetic stability. *Aicda*$^{-/-}$ iPSCs are genetically unstable; this may be an indirect effect due to failure in achieving the pluripotent ground state and therefore lacking genomic protection mechanisms. Alternatively, AICDA might regulate an intrinsic mechanism that is critical for maintaining chromosomal stability. AICDA KO mice are fertile, suggesting that AICDA mutant cells can achieve "naïve pluripotency" in vivo. We note that they generate small litters and are relatively inefficient for generating ESC clones [10]. Although the importance of AICDA in DNA demethylation during very early development has been shown [53], it seems likely that other mechanisms are able to compensate for the loss of AICDA in vivo. Although the requirement of AICDA for achieving the naïve pluripotent state may be most relevant in vitro, pluripotent cells are only maintained in vitro and are the main source of derivative cells that are used for various applications, for example, disease modeling, drug testing, and potential development of cellular therapies.

This report demonstrates a requirement for AICDA in regulating MAPK signaling. Besides being the master regulator of naïve pluripotency, MAPK signaling controls various biological processes including cell proliferation, differentiation, migration, and apoptosis. Here, we have been able to establish a link between two effectors of pluripotency, which should help in deciphering molecular networks controlling pluripotency, reprogramming, and differentiation. Moreover, the link between AICDA and MAPK signaling may shed light on the molecular basis of various cancers, both being strong drivers of oncogenesis.

Conclusion

AICDA is required for murine iPSCs to achieve the naïve pluripotent state during reprogramming. In the absence of AICDA, iPSCs can be stabilized as pluripotent cells, but they are similar to EpiSCs and are primed for differentiation. We conclude that hyperactive FGF/ERK signaling restricts AICDA-deficient iPSCs from achieving a naïve pluripotent state.

Acknowledgments

We are grateful to Bo Ding, Bonacept LLC., San Diego, for analyzing ERRBS data and preparing graphs and Kelly Banks, WCM, for performing gene expression cluster analyses. We are thankful to the laboratory of Jayanta Chaudhuri, MSKCC, for providing tail tips. The Epigenomics Core Facility of Weill Cornell Medical College carried out ERRBS and RNA-seq. WiCell Cytogenetics Laboratory, Wisconsin, performed G-banded karyotyping. This study was supported by a contract from the New York State Department of Health to T.E. (NYSTEM C029156).

Author Contributions

R.K.: conception/design, experimentation, data analysis, manuscript writing; T.E.: conception/design, data analysis, manuscript writing, financial support. Both authors gave final approval of the manuscript.

Disclosure of Potential Conflicts of Interest

The authors indicated no potential conflicts of interest.

Data Availability Statement

Raw RNA-seq data are available in a public depository, accession number: GSE129223. Raw ERRBS data are available in a public depository, accession number: GSE129223.

References

1 De Los Angeles A, Ferrari F, Xi R et al. Hallmarks of pluripotency. Nature 2015;525:469–478.
2 Takahashi K, Yamanaka S. Induction of pluripotent stem cells from mouse embryonic and adult fibroblast cultures by defined factors. Cell 2006;126:663–676.
3 Jaenisch R, Young R. Stem cells, the molecular circuitry of pluripotency and nuclear reprogramming. Cell 2008;132:567–582.
4 Mikkelsen TS, Hanna J, Zhang X et al. Dissecting direct reprogramming through integrative genomic analysis. Nature 2008; 454:49–55.
5 Chin MH, Mason MJ, Xie W et al. Induced pluripotent stem cells and embryonic stem cells are distinguished by gene expression signatures. Cell Stem Cell 2009;5: 111–123.
6 Guenther MG, Frampton GM, Soldner F et al. Chromatin structure and gene expression programs of human embryonic and induced pluripotent stem cells. Cell Stem Cell 2010;7:249–257.
7 Polo JM, Liu S, Figueroa ME et al. Cell type of origin influences the molecular and functional properties of mouse induced pluripotent stem cells. Nat Biotechnol 2010;28:848–855.
8 Martin A, Scharff MD. AID and mismatch repair in antibody diversification. Nat Rev Immunol 2002;2:605–614.
9 Bhutani N, Brady JJ, Damian M et al. Reprogramming towards pluripotency requires AID-dependent DNA demethylation. Nature 2010;463:1042–1047.
10 Kumar R, DiMenna L, Schrode N et al. AID stabilizes stem-cell phenotype by removing epigenetic memory of pluripotency genes. Nature 2013;500:89–92.
11 Milagre I, Stubbs TM, King MR et al. Gender differences in global but not targeted demethylation in iPSC reprogramming. Cell Rep 2017;18:1079–1089.

12 Habib O, Habib G, Do JT et al. Activation-induced deaminase-coupled DNA demethylation is not crucial for the generation of induced pluripotent stem cells. Stem Cells Dev 2014;23:209–218.

13 Shimamoto R, Amano N, Ichisaka T et al. Generation and characterization of induced pluripotent stem cells from Aid-deficient mice. PLoS One 2014;9:e94735.

14 Sommer CA, Stadtfeld M, Murphy GJ et al. Induced pluripotent stem cell generation using a single lentiviral stem cell cassette. Stem Cells 2009;27:543–549.

15 Nostro MC, Cheng X, Keller GM et al. Wnt, activin, and BMP signaling regulate distinct stages in the developmental pathway from embryonic stem cells to blood. Cell Stem Cell 2008;2:60–71.

16 Tsai SY, Maass K, Lu J et al. Efficient generation of cardiac purkinje cells from ESCs by activating cAMP signaling. Stem Cell Rep. 2015;4:1089–1102.

17 Gouon-Evans V, Boussemart L, Gadue P et al. BMP-4 is required for hepatic specification of mouse embryonic stem cell-derived definitive endoderm. Nat Biotechnol 2006;24:1402–1411.

18 Zhong X, Cui P, Cai Y et al. Mitochondrial dynamics is critical for the full pluripotency and embryonic developmental potential of pluripotent stem cells. Cell Metab 2018;29:979–992.

19 Anelli V, Villefranc JA, Chhangawala S et al. Oncogenic BRAF disrupts thyroid morphogenesis and function via twist expression. 2017;Elife, 6.

20 Akalin A, Kormaksson M, Li S et al. methylKit: A comprehensive R package for the analysis of genome-wide DNA methylation profiles. Genome Biol 2012;13:R87.

21 Pan H, Jiang Y, Boi M et al. Epigenomic evolution in diffuse large B-cell lymphomas. Nat Commun 2015;6:6921.

22 Chen CY, Morris Q, Mitchell JA. Enhancer identification in mouse embryonic stem cells using integrative modeling of chromatin and genomic features. BMC Genomics 2012;13:152.

23 Dowen JM, Fan ZP, Hnisz D et al. Control of cell identity genes occurs in insulated neighborhoods in mammalian chromosomes. Cell 2014;159:374–387.

24 Nichols J, Smith A. Naive and primed pluripotent states. Cell Stem Cell 2009;4:487–492.

25 Joo JY, Choi HW, Kim MJ et al. Establishment of a primed pluripotent epiblast stem cell in FGF4-based conditions. Sci Rep 2014;4:7477.

26 Shakiba N, White CA, Lipsitz YY et al. CD24 tracks divergent pluripotent states in mouse and human cells. Nat Commun 2015;6:7329.

27 Hayashi K, Lopes SM, Tang F et al. Dynamic equilibrium and heterogeneity of mouse pluripotent stem cells with distinct functional and epigenetic states. Cell Stem Cell 2008;3:391–401.

28 Brons IG, Smithers LE, Trotter MW et al. Derivation of pluripotent epiblast stem cells from mammalian embryos. Nature 2007;448:191–195.

29 Nussenzweig A, Nussenzweig MC. Origin of chromosomal translocations in lymphoid cancer. Cell 2010;141:27–38.

30 Chiarle R, Zhang Y, Frock RL et al. Genome-wide translocation sequencing reveals mechanisms of chromosome breaks and rearrangements in B cells. Cell 2011;147:107–119.

31 Ware CB. Concise review: Lessons from naive human pluripotent cells. Stem Cells 2017;35:35–41.

32 Lanner F, Rossant J. The role of FGF/Erk signaling in pluripotent cells. Development 2010;137:3351–3360.

33 Lake D, Correa SA, Muller J. Negative feedback regulation of the ERK1/2 MAPK pathway. Cell Mol Life Sci 2016;73:4397–4413.

34 Lee JY, Park S, Kim KS et al. Novel function of Sprouty4 as a regulator of stemness and differentiation of embryonic stem cells. Dev Reprod 2016;20:171–177.

35 Yang SH, Kalkan T, Morrisroe C et al. A genome-wide RNAi screen reveals MAP kinase phosphatases as key ERK pathway regulators during embryonic stem cell differentiation. PLoS Genet 2012;8:e1003112.

36 Choi J, Clement K, Huebner AJ et al. DUSP9 modulates DNA hypomethylation in female mouse pluripotent stem cells. Cell Stem Cell 2017;20:706.e7–719.e7.

37 Liu JW, Hsu YC, Kao CY et al. Leukemia inhibitory factor-induced Stat3 signaling suppresses fibroblast growth factor 1-induced Erk1/2 activation to inhibit the downstream differentiation in mouse embryonic stem cells. Stem Cells Dev 2013;22:1190–1197.

38 Zhang H, Gayen S, Xiong J et al. MLL1 inhibition reprograms epiblast stem cells to naive pluripotency. Cell Stem Cell 2016;18:481–494.

39 Factor DC, Corradin O, Zentner GE et al. Epigenomic comparison reveals activation of "seed" enhancers during transition from naive to primed pluripotency. Cell Stem Cell 2014;14:854–863.

40 Shaul YD, Seger R. The MEK/ERK cascade: From signaling specificity to diverse functions. Biochim Biophys Acta 2007;1773:1213–1226.

41 Ying QL, Wray J, Nichols J et al. The ground state of embryonic stem cell self-renewal. Nature 2008;453:519–523.

42 Schulz EG, Meisig J, Nakamura T et al. The two active X chromosomes in female ESCs block exit from the pluripotent state by modulating the ESC signaling network. Cell Stem Cell 2014;14:203–216.

43 Graf U, Casanova EA, Cinelli P. The role of the Leukemia Inhibitory Factor (LIF)—Pathway in derivation and maintenance of murine pluripotent stem cells. Genes (Basel) 2011;2:280–297.

44 Yang J, van Oosten AL, Theunissen TW et al. Stat3 activation is limiting for reprogramming to ground state pluripotency. Cell Stem Cell 2010;7:319–328.

45 Carcamo-Orive I, Hoffman GE, Cundiff P et al. Analysis of transcriptional variability in a large human iPSC library reveals genetic and non-genetic determinants of heterogeneity. Cell Stem Cell 2017;20:518–532 e519.

46 Murayama H, Masaki H, Sato H et al. Successful reprogramming of epiblast stem cells by blocking nuclear localization of beta-catenin. Stem Cell Rep 2015;4:103–113.

47 Teater M, Dominguez PM, Redmond D et al. AICDA drives epigenetic heterogeneity and accelerates germinal center-derived lymphomagenesis. Nat Commun 2018;9:222.

48 Tee WW, Shen SS, Oksuz O et al. Erk1/2 activity promotes chromatin features and RNAPII phosphorylation at developmental promoters in mouse ESCs. Cell 2014;156:678–690.

49 Hussein SM, Puri MC, Tonge PD et al. Genome-wide characterization of the routes to pluripotency. Nature 2014;516:198–206.

50 Weinberger L, Ayyash M, Novershtern N et al. Dynamic stem cell states: Naive to primed pluripotency in rodents and humans. Nat Rev Mol Cell Biol 2016;17:155–169.

51 von Meyenn F, Iurlaro M, Habibi E et al. Impairment of DNA methylation maintenance is the main cause of global demethylation in naive embryonic stem cells. Mol Cell 2016;62:983.

52 Giachino C, Orlando L, Turinetto V. Maintenance of genomic stability in mouse embryonic stem cells: Relevance in aging and disease. Int J Mol Sci 2013;14:2617–2636.

53 Santos F, Peat J, Burgess H et al. Active demethylation in mouse zygotes involves cytosine deamination and base excision repair. Epigenetics Chromatin 2013;6:39.

See www.StemCells.com for supporting information available online.